

Digital luminance photometry in the context of the human visual system

Sebastian SŁOMIŃSKI 

Warsaw University of Technology, Institute of Electrical Power Engineering, Lighting Technology Division, Koszykowa 75,
00-662 Warsaw, Poland

Abstract. Almost all solutions in modern lighting systems are based on LED technology. Luminance and obvious ease of control are the key characteristics of this light source. At the same time, luminances at the level of 10^8 cd/m² are a significant advantage of LED in design applications, where high luminous intensity amplification is important. However, in general and in road lighting applications, LED luminaires represent a source of potential discomfort glare. Unfortunately, lighting technology's metrology lags behind LED parameter development and optimization. The results of luminance measurements of the same luminaires, made with a luminance camera and meters with a measuring field, differ. The differences even appear for the same imaging luminance measuring devices with different lenses. This article presents the results of experiments and detailed analyzes related to modern digital luminance photometry based on the use of digital image sensors. Luminance tests were conducted on multi-source research models of luminaires. Traditional luminance measuring equipment with a measuring field was used in the experiment. The research was also supplemented with the measurements made using CCD/CMOS luminance cameras with selected components where the angular field of view of each pixel was a 0.45 min arc corresponding to the highest average human sight parameters. The results confirm that the average luminance value for multi-source luminaires depends on the measurement system configuration. It has been proposed to standardize the angular field of view parameters of all measurement systems, where the measurement aims to obtain a value that directly relates to human visual impressions (e.g. glare).

Key words: human vision; luminance distribution measurements; glare; lighting technology.

1. INTRODUCTION

Since the beginning of modern lighting technology development, photometric measurements have been important. The measurement methods began gaining key importance when modern simulation methods, forming the basis of lighting designing and optimizing processes [1], appeared. Digitally recorded luminous intensity distributions (LID) of light sources and luminaires are the starting point of a lighting design [2, 3]. Illuminance, luminance distributions, illumination uniformity and glare are calculated using digital IES, LDT or similar files. Typical construction of lighting devices with traditional light sources in terms of photometric features comprised two essential components: a light source and an optical system that most often was a mirror reflector. All these components had “macro” scale dimensions. In interior lighting, the solutions based on linear fluorescent lamps were dominant. The luminance of these lamps on a large surface of the tube did not exceed 50 000–100 000 cd/m². In these solutions, the LID has a “soft nature” (Fig. 1a, 1b). Additionally, luminance distribution on the entire surface of the reflectors and the light sources was uniform. High-luminance light sources such as halogen lamps, low and high-pressure sodium lamps and metal halide lamps have dominated in outdoor conditions. However, in most cases, luminaires

were equipped with large reflectors. Additionally, the former projects were implemented so that direct observation of the light source was not possible from the main illuminated directions. However, the appearance of LEDs has changed this situation. LEDs are excellent light sources that have completely revolutionized lighting perception [4].

Lighting has become more user-friendly, and control of luminous flux and light color has become cheap and simple. Easy and cheap lighting control options have been introduced, leading to significant energy savings [1, 5, 6]. However, the basic LED feature is high luminance [7], reaching the levels from several to hundreds of million cd/m² [8]. But, unlike traditional high-luminance light sources or COB LEDs, single power LEDs have relatively low luminous flux values, ranging from several to hundreds of lumens. This feature makes it necessary to build multi-source luminaires consisting of many chips covered with dedicated optical systems (Fig. 1c).

If we consider typical white LED systems used for lighting purposes, they are in 2 basic variants. As for interior lighting, a few dozen LEDs are often covered with a micro-prismatic structure or a diffuser to reduce luminance and glare. The situation is entirely different in the case of outdoor lighting, where it is necessary to obtain large luminous intensity amplifications. Due to the specificity of LED, reflector systems constitute a small percentage of the lighting solutions being designed, with lens systems/collimators being the dominant solution. This is because for this type of construction in the entire range of the illuminated space, it is possible to directly observe high lumi-

*e-mail: sebastian.slominski@pw.edu.pl

Manuscript submitted 2022-02-27, revised 2022-06-23, initially accepted for publication 2022-08-31, published in October 2022.

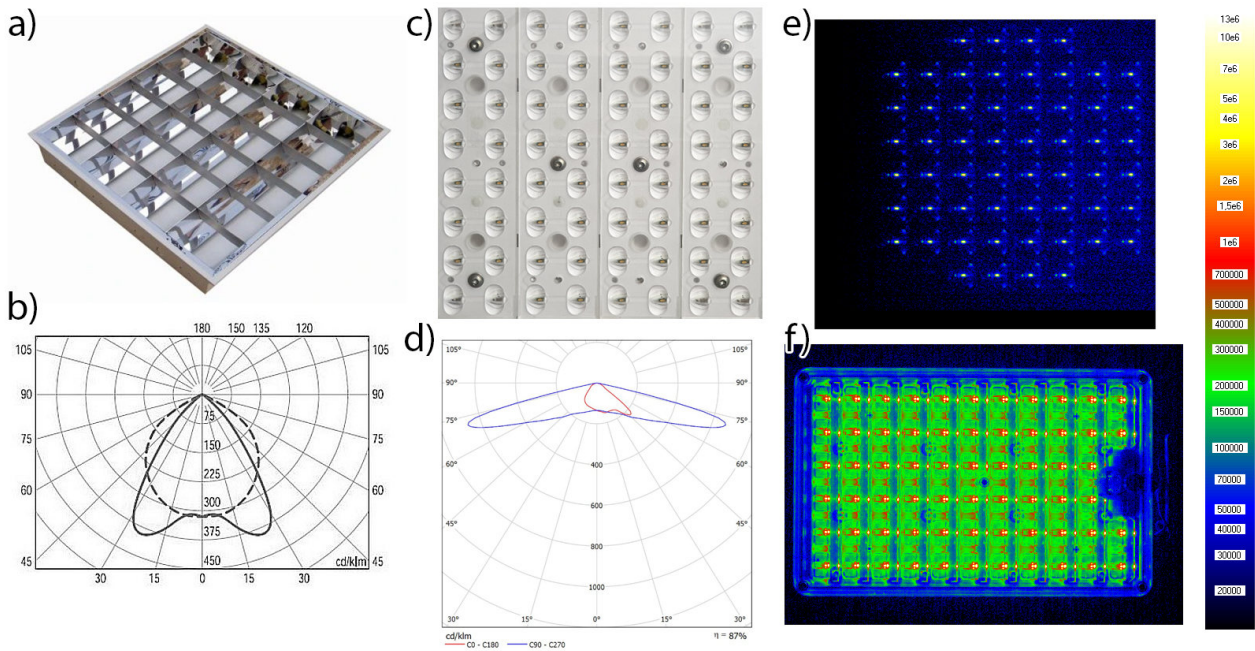


Fig. 1. Construction (a), (c), luminous intensity distributions (b), (d) and luminance distributions (e, f) of typical indoor and multi-source LED luminaires for road lighting

nance light sources (Fig. 1e, 1f). It has to be stressed that these features are associated with the possible potential for causing a glare phenomenon of considerable value.

1.1. Research area

The research aims to develop and verify the system guidelines that will enable objective measurements of luminance distributions, giving identical measurement results under the same lighting conditions. The research hypothesis based on the results of the research [8–10] has been clearly defined: each digital system for measuring ILMD luminance distributions shows a strong dependence of the average value of the recorded luminance on the measurement distance, i.e. the measurement field covered by a single photosensitive cell of the sensor [10]. For this reason, it is possible to develop guidelines that, after unifying the angular field of view of a single pixel, will make the results of measurements of luminance distributions identical, regardless of the components of the measurement system. The factors that directly affect the field of view of photosensitive cells are the photosensitive cells' physical dimensions and the lens's focal length. The unification of the angular field of view of the photosensitive cells of the sensor applies only to measurements of quantities that are directly related to the specific perception of light by the human eye, e.g. glare measurement.

Currently, the measurements of luminance distributions concern both the proper measurement of maximum and average values. The problems are generated by lighting devices having a large gradient of luminance variation. During research [10], it has been proved that the luminance value measured with imaging luminance measuring devices (ILMD) strongly depends on the sharpness of the measuring field and the angular field of view of individual sensor cells of the device. The current re-

search presented in this publication has confirmed this specificity. Additionally, it should be noted that another problem is the standardization of the entire design process, simulation calculations, and verification measurements related to lighting. The works known to date prove [11] that the values of lighting parameters related to the specificity of human eyesight differ from each other in the calculation of luminous parameters based on IES / LDT files and measurements using luminance meters with a measuring field and an ILMD. According to the author, the only possibility of obtaining full objectivization of the results of measurements of luminance distributions must lead to the standardization of measurement systems. That is, standardization of measurement systems not in the context of specific sensor parameters, but in the field of view (FOV) of individual photosensitive cells of different systems. FOV depends on the physical dimensions of the photosensitive cells and the focal length of the lens used. In the author's opinion, it would be most appropriate to link the FOV of the measurement system to the known average FOV of cones responsible for vision in humans.

The analysis of the angular field of view influence of individual photosensitive cells of ILMD on the recorded luminance value is discussed in this paper. The review of the literature of companies involved in the implementation of market-leading glare measurement devices [12] shows that there are no recommendations for selecting the focal lengths of lenses for ILMD sensors. The systems include the possibility to change the lens, which ultimately changes the angular field of view of the photosensitive cells of the sensor. This publication shows that this parameter significantly affects the value of the registered luminance in the case of luminaires with non-uniform luminance. Luminance underestimation increases with multi-source LED

luminaires. The key purpose of luminance measurements is to obtain a result consistent with the sensations of human eyesight. It should be added here that standardization should only cover the area of application where ILMD is used to measure parameters directly related to the specificity of human eyesight, for example, UGR (unified glare rating) measurement.

2. HUMAN VISION CHARACTERISTICS IN THE CONTEXT OF THE RESEARCH CONDUCTED

Luminance is the most important photometric parameter in lighting technology. For many years, this parameter has been measured very rarely due to the lack of precise and affordable measuring equipment. The situation has changed with the appearance of electronic luminance measuring devices with measuring areas similar to the world's dominant Konica Minolta "LS" device family. Modern measuring of luminance appears simple at first sight. It is sufficient to set the measuring device correctly and press the "start" button to get the result in cd/m^2 after a short while. In many cases, this is adequate, but there are more and more situations when such a simplified measurement is associated with significant errors.

When the measurement is performed to determine the luminance value of large and uniform surfaces, it is easy and thus mistakes can easily be avoided. Likewise, the case is similar when determining the luminance value of light sources for the purpose of designing e.g. optical systems of luminaires. To design optical systems for LEDs, luminance measurements are made from as short a distance as possible. The problem appears when luminance measurements are directly connected with the nature of the human eyesight and the brightness perceived by people, e.g. measurements and calculations of discomfort glare [8, 11]. That is why this paper concentrates on the measurements and calculations whose results and evaluation are directly linked to the human vision features (e.g. luminance distribution measurement for UGR calculation). Nowadays, it is often the common case that there is a discrepancy between the results of UGR values from a design, simulation calculations and the results of on-site measurements [10]. In order to assess the specific determinants and parameters of these differences, it seems necessary to briefly describe the nature of the human eyesight.

A human eye essentially consists of 2 receptor types, which are distributed over the retina (Fig. 2). Typically, an average of 92 million rods are responsible for night vision, whereas, 4.6

million cones [13] determine day vision at which both color vision and fine resolution of detail are available. Focusing on daytime vision and taking into account the number of photoreceptors, it is possible to combine these aspects to estimate a parameter such as resolution of human sight. If we consider the fact that the image is directed through the lens on the photosensitive area of the eye, just like in a camera, we can try to determine the angular field of view characteristic of each receptor on the retina.

In the publication "Human photoreceptor topography" [13] by Curcio, research on the spatial density of cones and rods on the surface of the retina for seven people aged between 27 and 44 is described. Depending on the age of the people in this study, large differences in the range of 4.08–5.29 million cones were observed. The average value of 4.6 million cones was assumed, the peak density of which was at the average level of 199 000 cones/ mm^2 . Large individual variability in the range of 100 000–324 000 cones/ mm^2 was also observed. The point of the highest density could be identified on the area of 0.032° . Density dropped rapidly and was lower by an order of magnitude at around 1mm beyond the central part. According to Williams [14], the minimum spacing between the rows of cones in the group of the researched people ranges from the 0.51 to 0.57 min arc, which corresponds to the density of 151 000 and 121 000 cones/ mm^2 , respectively. Taking into consideration different techniques for testing human eye parameters, the resolution of human eyesight covers a wide range from the 0.30 min arc to 0.89 and even a 1 min arc. All values are based on the average distance between the cones and the average distance of the retina from the optical center of the eye [15], on the topology of the retina [13] and on the research linked to the definition of visual acuity (VA) [16]. Therefore, the reference value accepted for the following studies is the mean value for the best vision of population with the Snellen visual acuity of 20/20 with Nyquist criterion stating that this corresponds to a detector resolution of at least 0.5 arcmin. A 0.45 min arc is this highest mean value resulting from the analyzed tests.

The resolution of the human eye is not identical for the entire population and individual human features have an impact on it. In addition, the human eye resolution is different for the central and peripheral field of view, depending on the density of receptors located on the surface of the retina. It is necessary to perform tests to find out what direct influence the field of view of photosensitive cells has on the luminance value perceived. It should be taken into account that the specificity of human vision is very complex and depends on many factors. The image is formed in the brain. The connections in the retina, between the photoreceptors and bipolar cells, and between bipolar and ganglion cells, are organized in so-called receptive fields to capture the dark-light transition more effectively. The receptive fields play an important role in contrast perception and visual acuity. In publication [17] the authors write that visual resolution decreases rapidly outside of the foveal center and that cone spacing, especially in the central fovea, is highly variable between individuals. Nevertheless, the only device that measures luminance in a similar way to the human eye is the luminance camera. Glare, an impression that is very individual and depends on

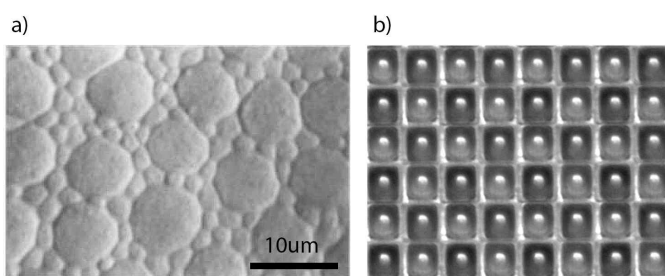


Fig. 2. Structure of the retina of the human eye (a) [13] and a typical CMOS sensor of the $6.45 \mu\text{m}$ size of a cell (b) [14]

a specific person, is assessed with the help of ILMD. Therefore, it is necessary to ensure that each ILMD system shows identical results under the same conditions. This will link indications and implemented calculations (UGR formula) with people’s feelings.

3. LUMINANCE MEASUREMENTS – STATE OF THE ART AND PROBLEMS

There are many interesting studies conducted in the world with regard to the adopted glare scale [18–20]. The results and recommendations for good practices are collected in publication [21]. Currently, the glare rating scale is based on the thresholds (levels of discomfort). These ranges are detailed by many researchers [19, 20, 22–24]. In each variant and in each study, the limits of glare occurrence come down to assigning subjective feelings to predefined intervals.

In the publication “Measuring Discomfort from Glare: Recommendations for Good Practice” [21], the authors wrote in relation to research connected with glare: “One reason why there is no agreed model is that there is a large variance in findings, both between subjects and between studies”. Of course, this applies to the subjective research that is done on the people participating in the experiments. That is why the above quoted opinion should be supplemented in the following manner: Until we have a measuring system that will ensure measurement results fully consistent with the results of design calculations and with the feelings of the people taking part in the research, it will be extremely difficult to achieve full compliance of the results between the respondents and the studies.

With the appearance of professional imaging luminance measuring devices whose construction is based on the use of digital image sensors in CCD or CMOS technology, making luminance measurements can be as precise as possible [25]. The traditional technology of constructing luminance meters (Fig. 3a) was based on the measurement of mean luminance values in a measuring field of a certain size.

Typically, the measurement area covered an angular area of 1/3°, 1°, 3°, or in the case of road lighting measurements, a rectangular area of 2' × 20'.

However, despite their undeniable advantages, these devices are not helpful for direct measurements of key parameters related to glare assessment such as UGR. The breakthrough came only when the equipment using digital sensors in CCD and CMOS technology for measurements appeared in the market. These devices can register luminance at many millions of points simultaneously, to some extent similarly to the way the human eye does. Two basic devices’ types dominate the market as far as digital luminance measurements are concerned:

- portable devices that use RGB cameras with color filters in the Bayer system [26],
- laboratory devices that have special constructions using gray matrices, without color filters.

In laboratory devices with mono sensors, spectral correction is performed using a dedicated $V(\lambda)$ filter placed between the lens and the sensor. The task of this filter is to adjust the silicon sensor’s spectral sensitivity to the human eye’s spectral sensitiv-

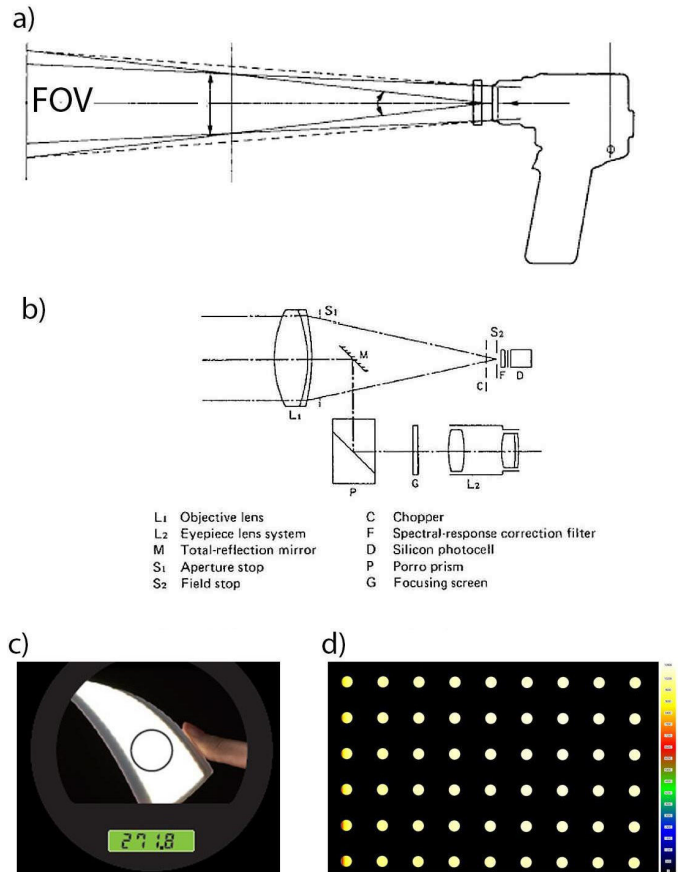


Fig. 3. Construction of luminance meters with a measuring field [24] (a), (b) and measurement result (c), result of ILMD measurement (d)

ity by the requirements of the CIE spectral luminous efficiency function $V(\lambda)$. In most market solutions, the signal from the sensor is converted into a digital form using 12-bit ADC converters. The image is most often projected onto the sensor with the help of rectilinear lenses.

The set of sensor + rectilinear lens enables precise calculation of the field of view of the entire sensor and the angular field of view of individual photosensitive cells (pixels) (formula (1)).

$$\text{FoV} = 2 \cdot \arctan \left(\frac{L}{F \cdot 2} \right), \quad (1)$$

where: FoV – field of view of individual photosensitive cells, L – diagonal dimension of the sensor, F – focal length of the lens.

Except for devices with rectilinear lenses, fisheye lenses are commonly applied in UGR measurements. An extremely wide field of view causes the extension of the field of view of individual pixels of the sensor, and thus can cause significant underestimation of the luminance value measured. The reason for this is the fact that when in the field of view of the camera there are multi-source luminaires (Fig. 1e, 1f), the luminance readout may be understated. The direct reason for this situation is presented in the later part of this publication and in articles [10, 27].

It is thus not surprising that many researchers are so eager to use ILMDs because they are undoubtedly the best measuring

devices in this field, capable of precisely measuring luminance in many millions of points within an instant. It should be appreciated that in her research [28], C. Villa applied measurement from the ILMD to determine background luminance value. In part of this work [28], it can be read that luminance measurement of the luminous parts of the luminaires was performed with a device with a physically applied Bayer filter and an extremely short fisheye lens.

In an interesting publication [29], in chapter 2.4, its authors report that the LED luminaire luminance was measured with a Radiant® Zemax ProMetric luminance camera. In another publication [30], a standard Canon EOS 5D Mark II with a 8mm lens was used to measure luminance. The system was calibrated based on comparing the measurement results for uniform areas with the measurement results received from the Minolta LS-110 device. In publication [20], extensive studies of the dependence of discomfort glare on small high-luminance light sources were performed, whereas the measurements were carried out with the help of two devices of a measuring field of (1/3° LS-110 and 1° LS-100) and with a DSLR Rebel T1i camera with a Canon 16-35 mm lens.

While analyzing the scientific articles, attention has been drawn to the fact that individual researchers use extremely different measurement configurations. It is very difficult to distinguish the details of the description of the parameters of measurement systems in scientific articles. The description of the system parameters is most often treated as marginal. Very often, it is not specified which variant of the device the authors used from many versions with different sensors and sets of lenses. Meanwhile, the selection of components has a direct impact on the luminance values obtained. Changing the lens to a lens with a different focal length will register different values of maximum and average luminance, especially for long-distance measurements [31]. Regardless of the luminance meters configuration, all measurements should give the same results.

Despite the widespread use of luminance cameras with silicon sensors in world science and technology, researchers use a wide variety of equipment. Research includes ready-made ILMD systems from companies such as Technoteam or Konica Minolta and ordinary DSLR digital SLR cameras calibrated for measurements by researchers themselves using a comparative technique with other reference luminance meters. Such systems do not have a correction to match the spectral sensitivity curve of the sensor to the spectral sensitivity curve CIE $V(\lambda)$ of the human vision.

It needs to be emphasized that the analysis and overview of the literature show that most researchers expect a stable system offering unambiguous measurement results. They do not want to deal with any measurement problems and measuring specification itself. It is understandable that luminance measurements should be as simple as possible. Adjusting the focus and pressing the “measure” button should give unambiguous and correct results in every situation. It is important in the case of the results that will have a direct impact on people’s subjective perceptions related to the luminance parameter and phenomena such as glare.

4. LUMINANCE CALCULATIONS AND MEASUREMENTS IN THE CONTEXT OF GLARE

To make an accurate assessment and find the cause of potential errors that may occur during calculations connected with lighting design, simulation calculations and measurement verification should be broken down into separate parts. This will be presented in this chapter.

4.1. Digital photometric data

Currently, each luminaire and most light sources available in the market offer photometric data. To prepare the IES/LDT files, a photometric darkroom, any goniometer and a lux meter are sufficient. However, documents in the IES/LDT formats of the most frequently used standards do not contain any luminance data. The luminance value of glare luminaires, e.g. for the UGR formula, is calculated from the luminous intensity value and the apparent surface area of the luminaires, which is calculated for the analyzed direction. Recalling the dependence for calculating the UGR (formula (2)).

$$UGR = 8 \log \left(\frac{0.25}{L_u} \sum_i \frac{L_i \omega_i}{P_i^2} \right), \quad (2)$$

where: L_u – background luminance (cd/m^2), L_i – luminance of the glare source “ i ” in the direction of the observer’s eye (cd/m^2), ω_i – solid angle of the glare source “ i ” seen from the observer’s eye (sr), P_i – position index (Guth’s index) for the glare source “ i ” (displacement from the line of sight).

The luminances of the luminous parts of all luminaires in the UGR dependence are described in [32].

$$L_i = \frac{I}{A_p}, \quad (3)$$

$$\omega_i = \frac{A_p}{r^2}, \quad (4)$$

where: I – luminous intensity in the direction of the observer’s eye (cd), r – distance from the center of the observer’s eye to the luminous parts of the luminaire (m), A_p – projected area of the luminaire (m^2).

The structure of files describing the photometric data of luminaires used for the UGR calculations includes data such as the number of light sources, the luminous flux of light sources, and key parameters: dimensions of the luminous luminaire surface and luminous intensity values in defined directions of the system (C, γ) or similar [11].

Therefore, where does the L_i luminance value necessary to calculate the UGR parameter value, which is the luminance of the glare light source towards the observer’s eyes, come from? Knowing that luminance is the quotient of the luminous intensity of the element and the apparent surface area of the component, which is seen from a given observation direction, the L_i value can be calculated based on the value. Here, however, the first problem appears. Regardless of the luminance distribution on the luminaires’ surface, the same luminous intensity distribution can be obtained.

This results in averaging luminance over the entire surface of the luminaires [10, 31]. This is not a problem for luminaires with uniform luminance over the entire surface (Fig. 3c), but it is essential for all luminaires with luminance distributions similar to Fig. 1.

It should be noted that more and more often light sources which are used for design purposes have very precise luminance models in the ISO TM25 standard (rayfile). With these models (Fig. 4), it is possible to perform very accurate simulations of reflector and lens systems using ray tracing methods. This format is commonly used to support the design of optical systems of lighting fixtures using Photopia, Speos, LightTools and similar software. Many companies have implemented these types of models in their software. Scientists [33, 34] have proposed effective simulation and measurement methods. But at present the TM25 format and similar formats are not used commonly to describe the photometric parameters of luminaires to be applied for indoor lighting simulation purposes. Additionally, to make the simulation calculations based on “rayfile” files, one should implement complex ray-tracing methods which are computationally demanding. All lighting design support applications like Dialux etc. are based on the use and simple implementation of photometric inverse square law instead of raytracing using luminance mapping.

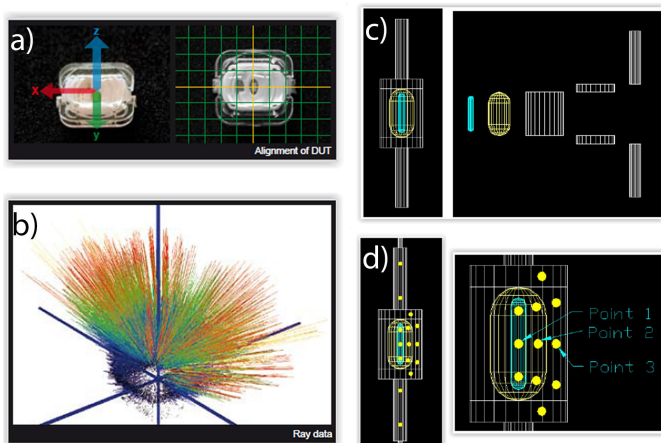


Fig. 4. An example model of the “rayfile” (a and b) and the structure of a light source model implemented in the LTI Photopia software (c and d)

4.2. Measurement of luminance parameters

Today, an ILMD is the only equipment that can measure the UGR directly. It should be taken into account that the ILMDs come in a very wide range of specifications. Individual devices differ in terms of the dimensions of the sensor and the number of pixels. In addition, it is possible to use many lenses with different focal lengths within one structure and this has a direct impact on the field of view of individual pixels of the sensor (formula (1)). That is why the simplest use of this type of device, limited to clicking the “start/measure” button, may be associated with massive errors in the case of measurements of parameters directly referring to the human vision nature. Currently the ILMDs constitute the sole alternative in the area of

luminance measurements. They are very advanced devices, offering great opportunities. However, it should be realized that they have specific characteristics that must be taken into consideration by the specialist when performing and processing the results of luminance distribution measurements.

In its rich publications, Technoteam, which is one of the pioneer companies in the field of constructing modern ILMDs, does not raise the problem of standardizing the angular parameters of [35] photometers in the context of UGR measurements. The other manufacturers [36, 37] also present different configurations which, after changing the lens, may give different luminance measurement results for multi-source luminaires.

The specificity of luminance measurements with all classic meters, such as the LS-100/LS-150 or similar, includes measurement of the mean luminance value inside a measurement field with a defined angular value (Fig. 3).

As far as the application of the ILMD is concerned, the result of measuring luminance distribution is the set of millions of averaged values for the angular field of view of each “pixel” recording local luminance values (Fig. 3d and Fig. 6). The average value from the defined measurement area similar to traditional equipment can be calculated in post-production on the basis of the data recorded while measuring.

Publication [35] relates to glare measurements using ILMD. This publication references the standard [38] which defines that “the luminance meter shall use a restricted total angle of the measurement cone to at least 0.03° in the vertical plane and at least 0.3° in the horizontal plane. If the ILMD determines the luminance for each grid point by averaging the reading of adjacent pixels, the mentioned limit angles shall not be exceeded”. The term “at least” means that without exceeding this threshold it is possible to use many systems, the field of view of which is significantly different from each other. For this reason, it is possible to obtain differences in luminance values for the same luminaires in the field of view of the photometers (Fig. 7).

In the CIE report [39] in relation to luminance measurements in chapter 4.5.4. with regard to ILMD, it is stated that “If an ILMD is used, its measurement uncertainty shall be verified by comparing the results for luminance distribution of a typical LED device measured with a discrete luminance meter”. Chapter 6 of report [39] describes the standard goniometric measurement and the luminance value obtained as a result: “average luminance is calculated by dividing the luminous intensity by the projected luminous area”. Additionally, it is described that “If the LED sources and LED luminaires have no diffusing covers and are observed as a sum of point sources (thus appearing as a mixture of luminous and non-luminous portions within the outer contour), method a) above for the determination of the average luminance from the luminous intensity in the viewing direction and the projected luminous area (the outer contour of the light output area) is not valid. For such LED devices, only measurements of the luminances of the luminous portions of the light output area are appropriate. Such measurements can be made using a luminance meter or an imaging luminance measurement device (ILMD)”. There is also no precise definition of the angular field of view of pixels of the measurement system, which consists of the physical dimensions of pixels and the focal length of the measurement lens.

The most extensive document on the subject of glare measurements, using modern digital luminance meters, is the CIE 232: 2019 document [40]. It is a much needed publication that puts in order the issues of modern glare measurements. Glare calculation procedures for large and small light sources are described. Additionally, much attention has been paid to LED luminaires that have non-uniform luminance distribution. A new formula has been proposed containing the correction factor “k” as a “uniformity correction parameter”. Information also appeared that: “The uniformity correction parameter, k, may be interpreted as a correction to the average luminance (as originally intended by Hara and Hasegawa), but also as a correction to the effective luminous area, a correction of the position index, or a correction of the whole term. The definition of the luminous part of the glare source has an impact on the average luminance value, the luminous area and the uniformity of the source. Therefore, the definition of the uniformity correction parameter “k”, must be based upon the definition of both the effective source area and the effective source luminance”. In the period of dynamic development of LEDs, these are very important proposals. On the luminance measurement issue it was written that “The resolution of this image needs to be sufficiently high to incorporate all relevant luminance variations” and “Either the measurement equipment is set to this resolution, or a finer resolution is used in the measurement and the image is blurred to the required resolution by applying a Gaussian filter”. However, the measurements (Fig. 8 and Table 2) show that the change in the angular parameters of the ILMD measurement system causes a large discrepancy in the maximum and mean values. This means that applying a Gaussian filter will not produce fully consistent results either. Therefore, it is necessary to conduct additional tests for carefully prepared measuring systems.

5. EXPERIMENT AND DESCRIPTION OF THE STAND

The aim of the experiment is to identify the dependencies of the parameters of the luminance measurement system, the type of luminance distribution on the surface of the luminaires and the recorded luminance values. Earlier studies have confirmed that there is a relationship between the depth of field of the ILMD measurement system and the angular field of view of individual photosensitive cells on the recorded luminance values [10, 27]. The following research aimed to show what differences are obtained and how to eliminate them.

In order to determine the detailed relationships between the luminance parameters for the same luminaires using different equipment and measuring techniques, a measuring stand was prepared.

This setup consisted of:

- a photometric darkroom,
- a 6 m long photometric bench,
- LMT luxmeter, which was used to measure luminous intensity from a distance of 9 meters for each variant of the apertures (accuracy $\pm 2\%$),
- Konica Minolta LS-100 camera with a measurement field size of 1° (accuracy $\pm 2\%$),

- LMT L1009 luminance meter with a measuring field size of $1^\circ, 3^\circ, 20', 6'$ (accuracy $\pm 2\%$),
- LMK imaging luminance measuring device with a $2/3''$ ICX285 sensor with resolution of 1392×1040 points, pixel dimensions: $6.45 \mu\text{m} \times 6.45 \mu\text{m}$ with a lens of focal length of 50 mm. Measuring accuracy $\Delta L < 3\%$ (for standard illuminant A) – $V(\lambda)$ and $f'1 < 4\%$.

For the purpose of the research, the models of luminaires were constructed (Fig. 5c) of dimensions $300 \text{ mm} \times 450 \text{ mm} \times 600 \text{ mm}$, with a measuring window of dimensions $225 \text{ mm} \times 350 \text{ mm}$. In each of the luminaire models there were light sources used, i.e. 6 pc's of 38 mm COB Citizen LEDs. The luminous flux that can be obtained from each of the diodes was 25 000 lm.

The author's own application and the ATmega 2560 microcontroller were used to control the luminaire. The system could make a smooth change of the luminance of the output surface of the luminaire in the range of $2000\text{--}25\,000 \text{ cd/m}^2$, with a uniformity of 0.94 (Fig. 5a). The spectral distribution of the LEDs used in the experiment is shown in Fig. 5b. All the devices used for measurements had $V(\lambda)$ spectral correction and worked in class A.

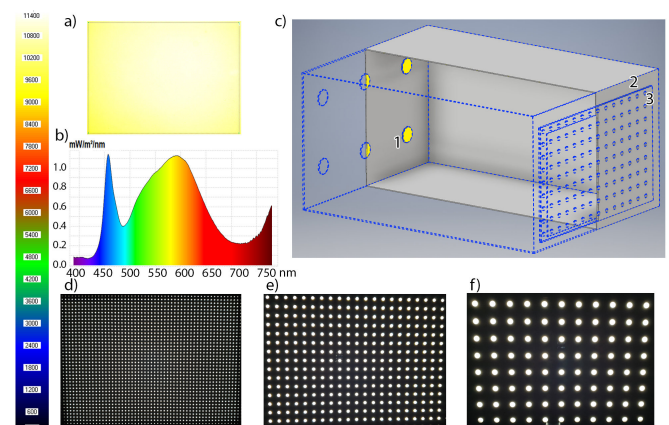


Fig. 5. Research model of luminaire, luminance distribution (a), spectral distribution (b), visualization of model (c), structure of openings/light source models (photos) (d–f)

Spot light sources were simulated by laser cutting of the openings in the surface of the black Plexiglas of 2 mm in thickness. A white diffuse plate illuminated directly by 6 COB light sources has been placed under the black Plexiglass. The dimensions of the openings and their spacing were selected on the basis of the assessment of these parameters for typical lighting solutions (Fig. 1c). 15 models of typical multi-source luminaires for outdoor lighting and 15 solutions for interior lighting were analyzed. The results indicate that $\times 3.2$ is typically the ratio of the distances between successive light sources as a function of their dimensions. For this reason, the distance between the centers of successive openings was assumed to be 3.2 times the dimension of the successive openings (Table 1).

The parameters of the openings were calculated so that from a distance of 3 meters the dimensions of the openings were covered by the angular field of view of 0.5 to 10 min arc (Table 1).

Table 1

Specification of luminaire models used in the experiment

	Diameter of openings (mm)	Distance between the centres of openings (mm)	Angular dimensions from distance of 3 m (min arc)
Aperture 1	0.44	1.4	0.5
Aperture 2	0.88	2.8	1
Aperture 3	1.75	5.6	2
Aperture 4	4.37	14	5
Aperture 5	8.70	28	10
White Acrylic	–	–	–

The positioning of the luminaires on the photometric bench was performed in such a manner that the minimum distance of the test luminaire from the measuring devices was 1.5 m, whereas the maximum distance was 6.7 m. Thanks to adjusting the distance, it was possible to obtain the conditions under which in extreme cases the surface area of a single luminous element was fully included in the angular field recorded by a single pixel of the imaging luminance measuring device sensor. With a measuring distance of 6.7 m, the field was 0.22 min arc (0.00366°).

Additionally, the focal length of the ILMD lens was selected so that with the known sensor dimensions of 2/3" and the known pixel dimensions of 6.45 $\mu\text{m} \times 6.45 \mu\text{m}$, the angular field of view of each pixel was obtained at a level close to 0.45 min arc. In the analyzed case, the assumed value was obtained as follows: for the smallest openings at a distance of 1.5 meters, the area covered by each individual pixel was that of 0.19 mm \times 0.19 mm. At the distance of 3.3 meters, the area covered by each individual pixel is that of 0.44 mm \times 0.44 mm. Finally, at a distance of 6.7 m, the area coverage is that of 0.85 mm \times 0.85 mm. At a measuring distance of 6.7 meters, the diameter of the smallest openings is twice smaller than the angular area covered by each pixel of the sensor of the ILMD set used in the experiment.

Figure 6 shows an exemplary location of the measurement zones covered by the angular field of view of the LS-100 and LMT L1009 devices in relation to the measuring field placed in the form of the area in the ILMD. The measuring fields were arranged in the central research area of COB luminaires. The re-

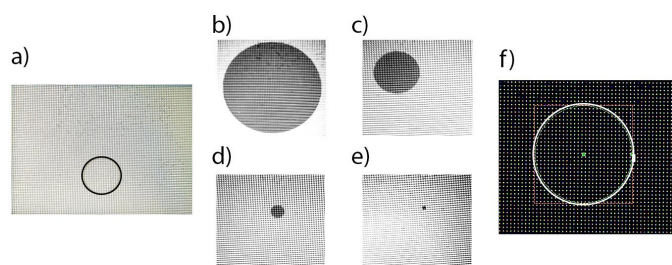


Fig. 6. Photos of the meter measurement fields LS-100 (a), L1009 (b–e), ILMD (f)

search was carried out in the photometric darkroom. All measuring devices were attached to special holders so that their lenses were located in the same place in the direction of the vector normal to the output surface of the tested luminaires. A Bosch GLL 3-80C cross laser was used for positioning the systems.

6. ANALYSES AND MEASUREMENT OF LUMINANCE

The introduction shows that for the purposes of different applications, the luminance value is calculated differently and based on different input data. As a result of all calculations, however, luminance distributions are not obtained, but the mean luminance value, characteristic of the entire luminous surface of the luminaires. Digital descriptions of luminaire parameters in IES/LDT or similar files are the starting point for all lighting simulation calculations.

As described earlier, luminance of the luminaires is determined on the basis of the luminous intensity values measured for the distance longer than minimal for photometric inverse square law and the apparent surface area of the luminaire which is calculated for the observation direction. In computational algorithms, this comes down to multiplying the area by the value of the cosine function for the observation direction. Luminance of the luminaires is calculated in this manner. To be aware of a chance of making a mistake, one can imagine a luminaire with a “checkerboard” structure where the black fields do not emit the luminous flux and the white fields emit it. The second variant is a luminaire of the same size as the “checkerboard” which is completely white, i.e. it emits the luminous flux with its entire surface. In both cases, the luminous surface area defined in the IES files will be identical. Both luminaires have the same luminous intensity. So, what will it change? Taking into account the fact that luminous intensity is the product of luminance and the luminous surface area, it turns out that in reality luminance values on the surface of the “checkerboard” will be twice higher than those on the surface of the luminaire uniformly emitting a luminous flux across the entire surface. However, luminance values for both of these variants calculated from the IES files will be identical.

Additionally, luminance distributions will also be the same in both cases and will be identical for a luminaire illuminating with its entire surface. We will receive the same dependencies for many variants of luminaires, including such an option in which the luminaire will have the entire center dark and will illuminate only circumferentially with the same luminous intensity as the two described earlier. Nevertheless, when luminance measurements are performed, the results obtained will depend on the part of such luminaires being covered by the imaging luminance measuring device.

For this reason, it was decided to carry out a number of tests and experiments different from those most often conducted in the context of discomfort glare. Much of the cited and very valuable research [18, 41–43] has been performed in a similar manner. The researchers prepare a test stand where a surface- or spot-illuminating luminaire in various configurations of lighting zones is placed. Then, a human sits down at the bench and

Digital luminance photometry in the context of the human visual system

assesses the perceived glare. The criterion is the dependence of the glare sensation as a function of the luminance value, luminance gradient and/or the spectral distribution of the light sources used. Everything in those investigations is conducted correctly. The only problem is that, for example, glare should be counted, measured and assessed objectively in addition to subjective judgments. These measurements are omitted. Nevertheless, there is no research that would link the luminance values obtained in various ways with the human sensations.

Research assumptions include the following points:

- luminance calculations on the basis of luminous intensity measurements – exactly as it is with the use of IES files,

- luminance measurements with two different measuring devices with an assumed measuring field,
- luminance distribution measurements with the ILMD, including the calculations of mean values from fields fitted to the measurement fields of traditional equipment.

All measurements were taken on the basis of the use of specially prepared, fully controlled luminaires whose construction is described in Section 5 and Table 1.

The analysis of luminance measurement results with the use of ILMD (Fig. 6 and Fig. 7) explicitly shows how the device “sees” luminance distribution. When the individual light sources included in the luminaire are so small that the field of

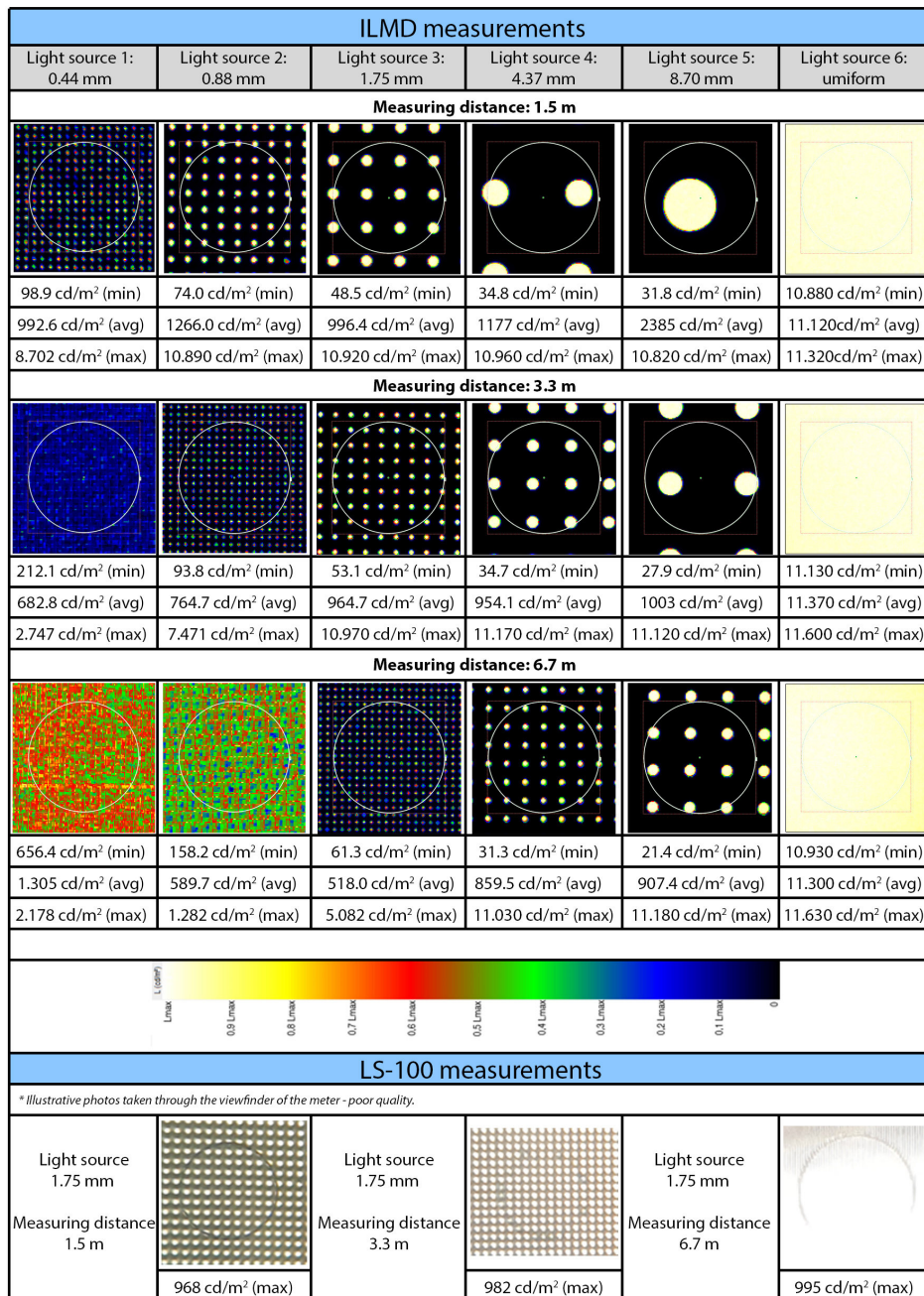


Fig. 7. Minimum/average and maximum luminance variability depending on light source dimensions and measurement distance

view of a single pixel covers them completely and when their high luminance is surrounded by very low background luminance, the individual pixels record the average luminance from their field of view. The presented results show clearly that under the conditions when the dimensions of the light sources are close to the angular field of view of the pixels, the device is not able to separate them and some significant disturbances of the recorded luminance values appear. These disturbances are unpredictable.

In Fig. 8, for a luminaire that consists of light sources of a diameter of 0.44 mm, with distances between the light sources of 1.4 mm, with measuring distance of 6.7 m, the mean luminance value exceeding the average values for all measurements and all measuring devices was obtained. There is also a noticeable impact of high point luminance on the signal triggering the neighboring pixels of the sensor. The most stable indications for each of the analyzed variants were obtained with the use of the Minolta LS-100 camera with the 1° measuring field. Therefore, this device will be treated as a reference one. It is worth noticing that the device indications correspond to the mean luminance calculations made for the luminaires with the use of inverse square law formula and (Table 2) thus most accurately. At the same time, for the above reasons these results cannot be treated as objectively the best and most closely correspond-

ing to the sensations registered by the human sight. At the moment it is not clear which of the devices can generate the results which correspond to the human luminance sensations. This idea will be developed in the summary of this paper.

6.1. Dependence of luminance value as function of measuring distance

The analysis of the recorded luminance values for subsequent models of luminaires (Fig. 8), where the measuring distance is a variable, shows two regularities. The first one is the fact that the value of the mean luminance recorded with the Minolta LS-100 luminance meter with the measuring area of 1° is the closest to the mean luminance value calculated on the basis of the luminous intensity measurements for the entire surface of the luminaire models. The calculations were made in the same way as they are made on the basis of digital IES/LDT files. For the light sources with a diameter of 0.44 mm, average luminance values were successively obtained as follows: for a distance of 1.5 m: 1163 cd/m² (LS-100) and 1343 cd/m² (calculations), for a distance of 3.3 m: 1259 cd/m² (LS-100) and 1343 cd/m² (calculations), for a distance of 6.7 m: 1310 cd/m² (LS-100) and 1343 cd/m² (calculations). Similarly, for the same parameters, the ILMD recorded the mean luminance values from the analogous measuring field as follows: 992 cd/m² for the measur-

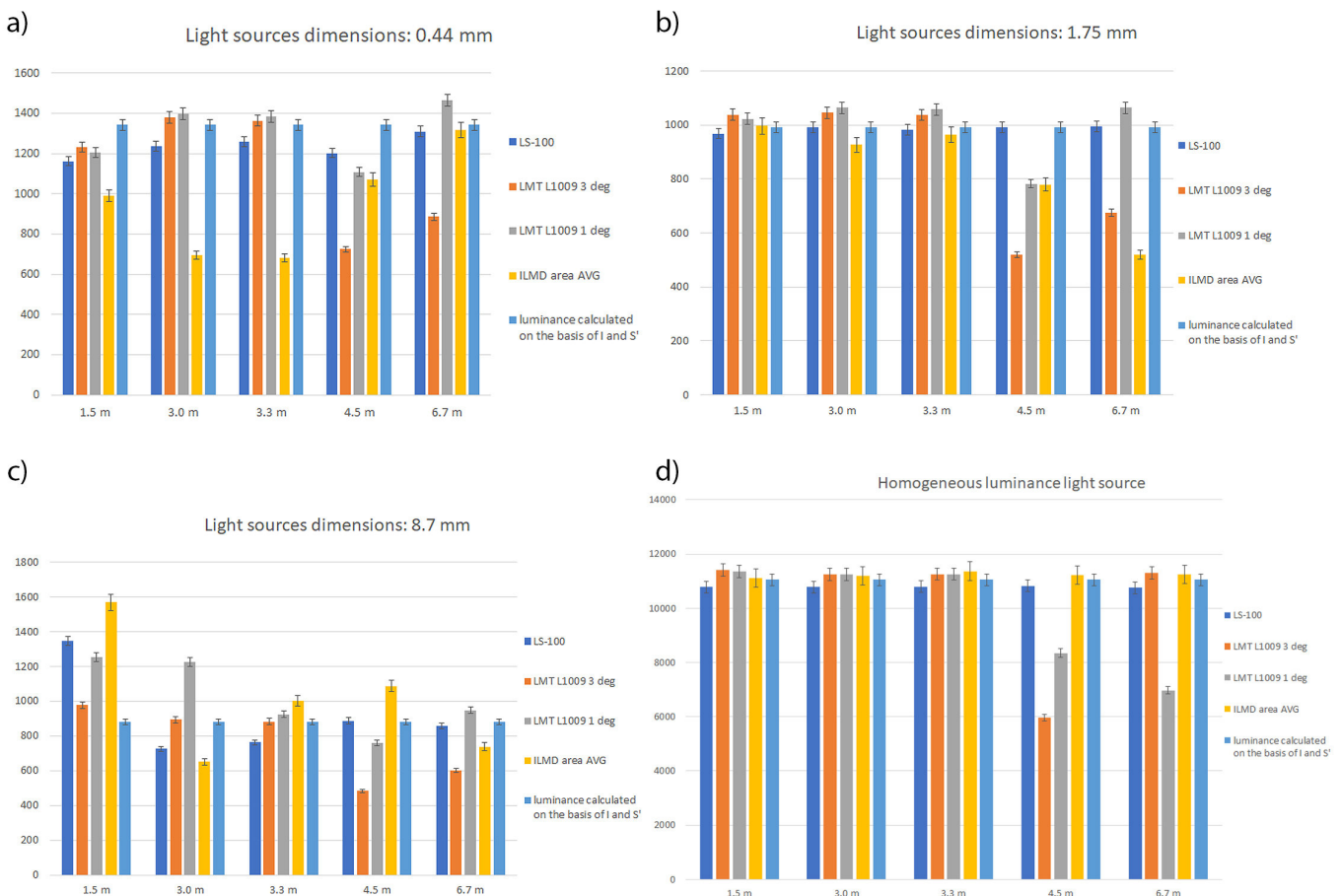


Fig. 8. Dependence of luminance value as function of measuring distance for variable light source dimensions (a–c) and for homogeneous luminance light source (d)

ing distance of 1.5 m, 682 cd/m² for 3.3 m and 1318 cd/m² for 6.7 m. The luminance values for the subsequent models of luminaires are presented in Table 2.

The detailed analysis of the results shows that the values calculated on the basis of the LID of the luminaires and the re-

Table 2 [cont.]

Table 2

Dependence of luminance value (cd/m²) as a function of the measuring distance for 6 dimensions of light sources models

	Measuring distance	1.5 m	3.0 m	3.3 m	4.5 m	6.7 m
0.44	LS-100	1163	1235	1259	1203	1310
	LMT L1009 3 deg	1233	1381	1364	725	886
	LMT L1009 1 deg	1205	1398	1385	1109	1467
	LMT L1009 20'	1226	1395	1393	1400	1493
	LMT L1009 6'	1243	1439	1415	1414	1457
	ILMD area MIN	98	177	212	295	619
	ILMD area AVG	992	696	682	1072	1318
	ILMD area MAX	8702	3016	2747	2573	2178
	luminance calculated on the basis of I and S'	1343	1343	1343	1343	1343
	0.88	LS-100	1181	1218	1220	1206
LMT L1009 3 deg		1251	1316	1302	681	844
LMT L1009 1 deg		1258	1330	1324	997	1349
LMT L1009 20'		1259	1310	1308	1247	1373
LMT L1009 6'		1235	1315	1342	1280	1375
ILMD area MIN		74	90	93	132	273
ILMD area AVG		1266	856	764	611	586
ILMD area MAX		10890	8099	7471	3795	1175
luminance calculated on the basis of I and S'		1262	1262	1262	1262	1262
1.75		LS-100	968	991	982	991
	LMT L1009 3 deg	1038	1045	1037	520	675
	LMT L1009 1 deg	1023	1064	1057	782	1064
	LMT L1009 20'	1031	1036	1055	962	1069
	LMT L1009 6'	1210	932	1064	998	1030
	ILMD area MIN	48	51	53	55	67
	ILMD area AVG	996	926	964	779	519
	ILMD area MAX	10920	10830	10970	9183	4839
	luminance calculated on the basis of I and S'	991	991	991	991	991
	4.37	LS-100	725	852	902	883
LMT L1009 3 deg		930	924	921	456	627
LMT L1009 1 deg		860	974	897	608	925
LMT L1009 20'		1320	993	933	767	1012
LMT L1009 6'		1460	2190	1155	878	284
ILMD area MIN		34	32	34	31	33
ILMD area AVG		1177	677	954	932	929
ILMD area MAX		10960	11070	11170	11020	10870
luminance calculated on the basis of I and S'		904	904	904	904	904

	Measuring distance	1.5 m	3.0 m	3.3 m	4.5 m	6.7 m
8.70	LS-100	1346	725	762	887	857
	LMT L1009 3 deg	976	893	882	483	602
	LMT L1009 1 deg	1252	1225	924	760	947
	LMT L1009 20'	5300	17	149	980	1003
	LMT L1009 6'	5100	10	10	963	11
	ILMD area MIN	27	27	27	24	12
	ILMD area AVG	1567	650	1003	1087	738
	ILMD area MAX	10840	11070	11120	11140	11080
uniform	luminance calculated on the basis of I and S'	881	881	881	881	881
	LS-100	10780	10790	10800	10830	10760
	LMT L1009 3 deg	11420	11250	11260	5970	11310
	LMT L1009 1 deg	11360	11250	11260	8350	6970
	LMT L1009 20'	11370	11260	11260	10480	11360
	LMT L1009 6'	11340	11250	11240	10700	11310
	ILMD area MIN	10880	10930	11130	10910	10920
	ILMD area AVG	11120	11200	11370	11230	11260
	ILMD area MAX	11320	11470	11600	11500	11590
	luminance calculated on the basis of I and S'	11054	11054	11054	11054	11054

sults of measurements using the Minolta LS-100 device fluctuate around similar values. Additionally, the measurement results are stable for a given distribution of light sources on the surface of luminaires regardless of the measuring distance.

Similarly, as for the surface of a single luminaire where the entire light source represents its entire surface, the results are stable and very consistent (LS-100: approx. 10 800 cd/m², calculations: 11 054 cd/m²). In this case, the results of measurements with the ILMD are also very close to those obtained with other methods and fluctuate around the value of 11 230 cd/m². The situation changes for a different structure of the light source system dramatically (Table 2).

For light sources of a diameter of 0.44 mm and depending on the measuring distance, the ILMD records the following average luminances: 992 cd/m², 696 cd/m², 682 cd/m², 1072 cd/m², 1318 cd/m² (for the consecutive distances: 1.5 m, 3.0 m, 3.3 m, 4.5 m, 6.7 m). Thus, all mean values are lowered as compared to the two remaining methods and there is no regularity in the direction of changes in the results. The measurement results are presented in Table 2 and Fig. 8. For the consecutive luminaires, we can distinguish the regularity that for the shortest measuring distance the values recorded with the ILMD are higher than in the other methods, and the values decrease as the device is moved away from the luminaire. The most interesting results have been observed for the smallest light sources whose size is within in the field of view smaller than approx. 1 min arc. Regardless of the measuring distance, the recorded mean luminance values are even 50% lower than the values measured with the LS-100 device and those calculated on the basis of the LID.

6.2. Dependence of luminance values on angular dimensions of light sources

In another part of the experiment, it was investigated whether at a stable measuring distance the recorded mean luminance values behaved as a function of the changes in angular size of light sources steadily and predictably (Table 2). The analysis was carried out for 3 measuring distances: 1.5 m, 3.3 m, and 6.7 m. Except for one disturbance of the result for the distance of 1.5 m, for the LS-100 device and the largest light sources, the results of the LS-100 measurements again coincide with the calculation results for all consecutive conditions (Fig. 9). Meanwhile, the ILMD measurements for the smallest light sources and the measuring distance of 1.5 m fluctuate around the value of 1000 cd/m², without maintaining the change trend corresponding to the calculations. At a distance of 3.3 m, the direction of changes in the luminance value from the ILMD is opposite to the others. For the distance of 6.7 m, the correctness and relationship with the calculated values cannot be distinguished either. In the LMT L1009 measuring device, one can notice the recorded luminance value's dependence on the measuring distance function. Especially after exceeding the distance of 3.3 meters (for 4.5 m and 6.7 meters), luminance drops appear that do not follow the trend of changes in luminance registered with LS-100 and the values resulting from the calculations. Additionally, the LMT results are not consistent with the results of measurements with the use of other devices

and calculation methods. Because, e.g. the luminance value for a 1.75 mm light source is stable for the distance of 1.5–3.3 m, then it drops by almost a half for the measuring field of 3 degrees and the distance of 4.5 m, and then increases for the distance of 6.7 meters. For this reason, these results are provided for illustrative purposes only and were not considered in the discussion of the results. It should be mentioned that the device was operational and had a valid verification certificate. The second phase of the experiment is currently being investigated. It provides for the participation of 80 respondents. Therefore, these results may prove valuable shortly. Considering the high variability of the ILMD indications, the use of this equipment for universal measurements of parameters similar to the UGR is currently disputable. According to the author, further research and complete standardization of measuring equipment with digital CCD/CMOS sensors for measuring parameters directly related to the nature of human vision nature are necessary.

When luminaires having uniform luminance distribution, e.g. those with diffusers, are in the field of view of the measuring device, measurement results will be stable and objectively correct. However, when in the field of view there is a luminance gradient changing the appearance of the luminaire to one similar to that of multi-source luminaires (Fig. 1c and Fig. 5d–5f), the results of the measurements and, consequently, of the luminance calculations for glare sources (L_i in UGR formula) will be imprecise (formula (3)). However, the most significant com-

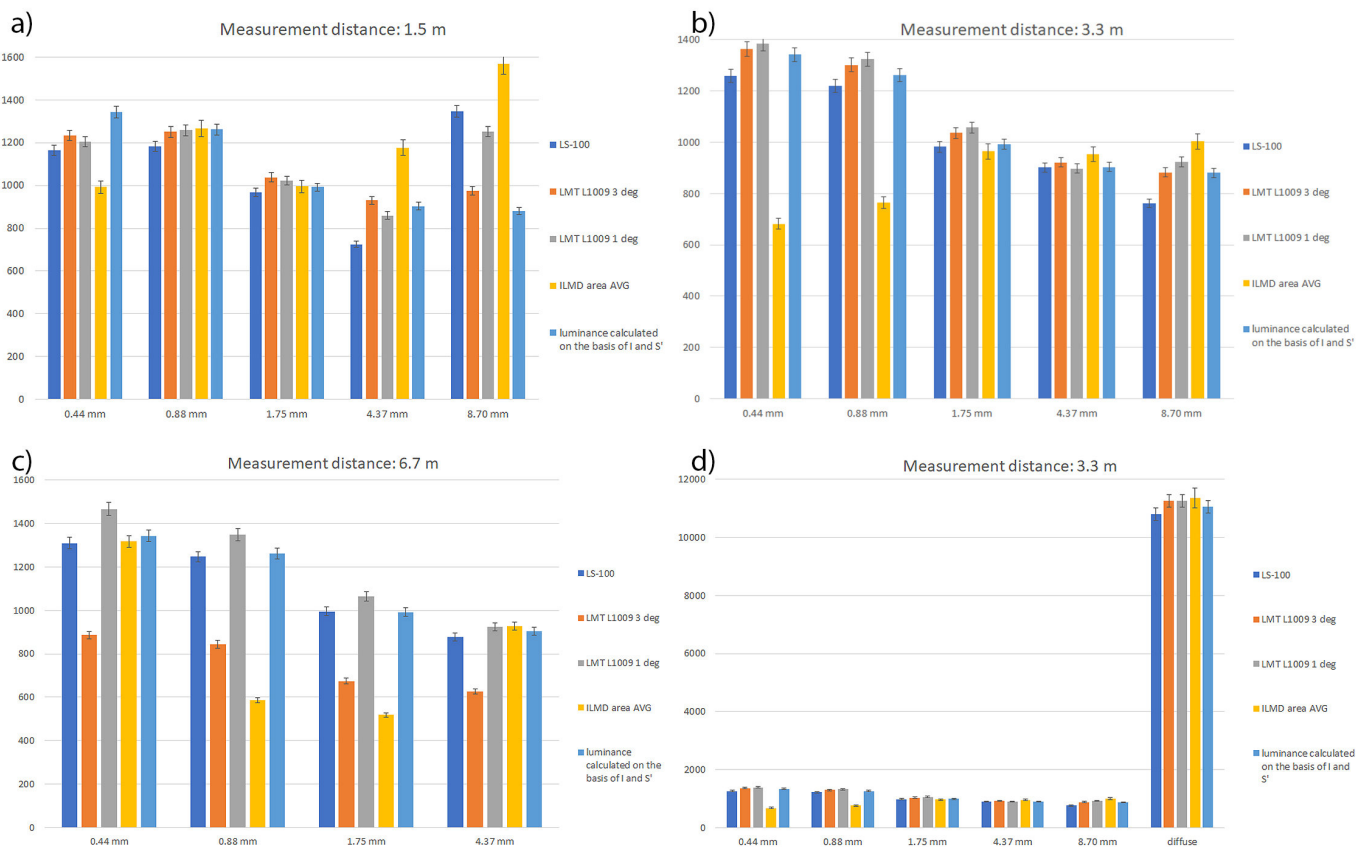


Fig. 9. Dependence of luminance values on angular dimensions of light sources at a constant measuring distance without uniform luminaire (a–c) and with uniform luminaire (d)

plication is introduced by the fact that the direction of the error will not be known. It is not clear whether the results will be overestimated or underestimated.

For research purposes, changing the measurement field covered by a single pixel can be done in two ways. One is to change the distance of the invariant sensor system and the prime lens from very small angular light sources. The second is the change of the focal length value with the system measuring distance unchanged. By “small light sources”, it is meant that they are those with dimensions that oscillate angularly around the area encompassed entirely by a single photosensitive cell of the sensor.

The conducted research shows that by increasing the measuring distance from the models of multi-source luminaires with small angular light sources, the maximum value and average value of the registered luminance in most cases decreases (Table 2). The same happens when the focal length is changed to a smaller one [10]. Therefore, two ILMD systems, differing in the resolution of the sensor or the focal length of the lens, which will be used for UGR measurements, will give different measurement results [11]. This is due to the different luminance values of the L_i dazzling luminaires (formula (3)). The result of the background luminance measurement L_u (formula (2)) will be the same because the luminances of large homogeneous surfaces are independent of the angular field of view of light-sensitive cells and the measurement distance (Fig. 8d). Therefore, the factor causing measurement discrepancies should be eliminated by standardizing a single photosensitive cell’s angular field of view, regardless of the ILMD system components used.

The results presented in Figs. 8 and 9 show that when the area covered by a single pixel is similar, the luminance values obtained will also be similar. For example, for light sources with the size of 0.44 mm and the measuring distance of 1.5 m, the value of $L_{\min} = 98 \text{ cd/m}^2$, $L_{\max} = 8702 \text{ cd/m}^2$, $L_{\text{avg}} = 992 \text{ cd/m}^2$. When the measuring distance increases in proportion to the increase in the size of the light sources, we obtain for 0.88 mm and 3.0 m the values of $L_{\min} = 90 \text{ cd/m}^2$, $L_{\max} = 8099 \text{ cd/m}^2$, $L_{\text{avg}} = 856 \text{ cd/m}^2$. However, when the measuring distance increases from 1.5 to 3.0 m but the dimensions of the light sources do not increase, for 0.44 mm and 3.0 m we obtain $L_{\min} = 177 \text{ cd/m}^2$, $L_{\max} = 3016 \text{ cd/m}^2$ and $L_{\text{avg}} = 696 \text{ cd/m}^2$.

In addition, the maximum value of luminance corresponding to the reality for the homogeneous variant is obtained only when the angular field of view of at least one pixel of the sensor fits entirely within the size of the light source. It should be noted that the maximum values, oscillating around 11 000 cd/m^2 , are obtained for a source with the dimensions of 0.88 mm and only one distance of 1.5 m. The same maximum value in other cases is recorded for a light source with the dimensions of 1.75 mm for the distance of 1.5–3.3 m, a light source with dimensions of 4.37 mm for a distance in the range of 1.5–6.7 m and for a light source of 8.7 mm in the whole range. For light sources with the dimensions of 0.44 mm for the used configuration of the measurement system (reference to the ILMD configuration and the lens), the real maximum value is not obtained for any measurement distances. This is because the field of view of a single

photosensitive cell is not fully contained in the light source’s dimensions. The cell measures the average value of luminance of the light source and the immediate surroundings. In this case, all maximum values are understated.

7. FURTHER RESEARCH

Based on the presented analyses and the research [8–10, 29], it can be concluded that currently the ILMD technology is very advanced, however, it requires standardization. When the devices are used to measure real luminance values from short measuring distances, or with the use of lenses of large focal lengths exceeding 50–100mm, the operator of the equipment obtains a lot of precise information related to luminance distributions. However, if the measurements are connected with the assessment of parameters resulting from the human sight nature, it is necessary to standardize the measuring equipment and expand the files to include photometric data of luminaires (IES/LDT/etc.).

These files are sufficient for calculations related to the distribution of illuminance and luminance on the illuminated surfaces. Nevertheless, at least for one direction of observation, $\gamma = 0^\circ$ and the assumption of the Lambertian nature of the luminance distribution, it is necessary to supplement their structure with a simplified luminance distribution on luminaire surface. The division of the luminaire into e.g. 1000 to 10 000 parts, where the luminance value will be saved, can easily be added to the IES/LDT files. This can also be done without significantly increasing the file size. However, it will then become possible to make more precise UGR parameter calculations that will overlap with the results of ILMD measurements and the lighting users’ feelings.

The test results show that under the presented conditions the values recorded with the ILMD differ from both the values recorded with the devices with a measuring field and from the calculation results based on the luminous intensity and apparent surface area of the luminaire. To determine which results are closer to people’s subjective assessments, additional studies are currently being carried out with respondents. The human eye is a very complex “measuring device”. Taking into account its structure and principle of operation, the ILMDs are theoretically the closest to the human eye. The human eye reacts to a sensor in a similar manner and it consists of millions of receptors working with the lens. Each light-sensitive cell records the mean luminance for a given angular area. Human eye adaptation applies to the entire eye, like a change in exposure time in the ILMD.

Nevertheless, the human vision parameters which are dependent on personal and genetic characteristics fluctuate around the values in the range of 0.3 to 1 min arc. Meanwhile, parameters such as the field of view of the ILMD set or a single photosensitive cell are subject to great variability depending on the configuration of the measuring system. The key elements of luminance camera configuration include e.g. parameters such as physical size, number of pixels, pixel dimensions for a sensor and focal length, optical resolution of the lens, etc., for other system components. Therefore, in-depth understanding of the

specificity of ILMD operation in direct relation to people's sensations is so important in order to develop a system that will be characterized by the corresponding results of design calculations, simulations and measurements.

The results presented in this publication clearly show that the luminance measurement result strongly depends on the configuration of the measurement system for the same variants of lighting fixtures.

8. SUMMARY AND CONCLUSIONS

The human eye is a complex "measuring device". During the measurements, the luminance perceived by the eye is translated into numerical values which are then used for calculations. The author of this publication, apart from purely academic activity, deals with designing optical systems for luminaires and developing measuring equipment. The results of research [8, 10, 44] and [45] indicate that it is necessary to design measurement systems that deliver results which are consistent, under all conditions, with people's impressions. The key issue is to adjust the measurement system to the human sight nature. Citing C.A. Curcio: "There are several estimates for the maximum density (or minimum spacing) of cones in the adult fovea (Osterberg, '35; Hartridge, '50 [46]; O'Brien, '51 [47]; Miller, '79 [48]; Farber *et al.*, '85 [49]; Yuodelis and Hendrickson, '86 [50]; Ahnelt *et al.*, '87 [51]), which range from 49 600/mm² (Farber *et al.*, '85 [49]) to 238 000/mm² (Ahnelt *et al.*, '87 [51]). These studies focus on a variety of histological techniques and a range of ages, and many of these studies are based on only one or two eyes". There is not and cannot be one unquestionable numerical value characteristic of the resolution of human sight. The values calculated with various methods cover the range from 0.3 to 1 min arc. This publication presents the analysis of the results of luminance calculations and measurements for different methods. The focus was on the ILMD system configured so that the angular field of view of a single photosensitive cell was equal exactly to the highest average resolution of human vision, shown in most studies as 0.45 min arc. The measurements were taken for specially designed luminaires in which the light source dimensions of 0.44 mm, 0.88 mm, 1.75 mm, 4.37 mm and 8.70 mm consecutively ensured the coverage of the angular area corresponding to a 0.5, 1, 2, 5 and 10 min arc from 3 m of distance.

The first method of luminance determination was the computational method used in photometry for laboratory measurements of luminous intensity distributions of luminaires for the needs of e.g. digital IES/LDT or similar files. It is based on measuring the value of the luminous intensity for the distance further than minimal for photometric inverse square law. Taking into account the apparent luminous surface of the luminaires, mean luminance value was calculated. The second method for indicating the luminance value was the method of direct measurements using two devices with a measuring field. These devices were Minolta LS-100 and LMT L1009. The third method was based on the ILMD system with a 2/3" ICX285 sensor and a lens selected so that the field of view of each pixel was a 0.45 min arc.

By analyzing the obtained results from publication [8, 10] and [31], one can defend the hypothesis that it is possible to develop guidelines that, after unifying the angular field of view of a single pixel, will make the results of measurements of luminance distributions identical, regardless of the components of the measurement system used.

The results of the experiment show clearly that when the individual light sources are so small that the field of view of a single pixel covers them entirely, individual pixels record average luminance from their field of view. Typically high-luminance light sources are surrounded by background luminance of a very low value (Fig. 1e), therefore the recorded luminance value is very low as compared to the average luminance value for the light source itself.

This publication presents the research results and highlights the need for standardization of measurements and luminance description in digital files with photometric data used to calculate parameters such as UGR. Additionally, it is recommended that each time a detailed specification of the measuring equipment and the measuring distance be provided. In the case of scientific publications and the evaluation of parameters such as e.g. UGR, the conversion value of the angular field of view for each CCD/CMOS sensor cell used in the measurement system should be included in the measurement protocol. This will allow to provide comparable test results connected with glare. Otherwise, we will not have any modern measure of description of glare sensations, fully coinciding with the results of calculations and laboratory measurements.

Standardization of the measurement system configuration must mean moving away from defining parameters as "at least" and replacing them with a specific value such as 0.45, 0.5 or 1 min of arc, which will have to be realized by the equipment manufacturers. Providing one specific field of view for each "pixel" is possible by adjusting the lens and by ensuring precisely adjusted focal length for the physical dimensions of the photosensitive cells of the sensor. Publication [10] shows that the angular field of view of individual photosensitive cells of the sensor is of key importance in the case of recording the luminance distributions of multi-source luminaires. It is influenced by averaging the luminance of light sources and their surroundings by individual photosensitive cells. The change in averaged values does not coincide with the change recorded by traditional measuring instruments (Fig. 9c). However, in the case of traditional measuring instruments, the field of view of the devices usually covers 1st degree or 3 degrees as standard. In the case of ILMD for the same sensor, the use of a lens with a different focal length radically changes the system parameters. Knowing the technical limitations and the ratio of resolution to matrix dimensions, it is recommended to quickly adopt the standardization of all systems dedicated to measuring parameters such as GR or UGR so that the field of view of individual photosensitive cells does not exceed 1 arc minute.

9. PATENTS

The solution described in the article is subject to patent protection No. PL 231114 "Method for measuring the luminance

distribution and the system for measuring the luminance distribution”.

ACKNOWLEDGEMENTS

The author would like to thank the Authorities of the Electrical Power Engineering Institute (Warsaw University of Technology) for the financial support as regards language proofreading and open access publication.

REFERENCES

- [1] T.W. Kruisselbrink, R. Dangol, and E.J. van Loenen, “A comparative study between two algorithms for luminance-based lighting control,” *Energy Build.*, vol. 228, p. 110429, 2020, doi: [10.1016/j.enbuild.2020.110429](https://doi.org/10.1016/j.enbuild.2020.110429).
- [2] D. Mazur, H. Wachta, and K. Leško, “Research of cohesion principle in illuminations of monumental Objects,” in *Analysis and Simulation of Electrical and Computer Systems. Lecture Notes in Electrical Engineering*, 2018, vol. 452, Springer, Cham. pp. 395–406, doi: [10.1007/978-3-319-63949-9_26](https://doi.org/10.1007/978-3-319-63949-9_26).
- [3] P. Pracki and K. Skarżyński, “A Multi-Criteria Assessment Procedure for Outdoor Lighting at the Design Stage,” *Sustainability*, vol. 12, no. 4, p. 1330, Feb. 2020, doi: [10.3390/su12041330](https://doi.org/10.3390/su12041330).
- [4] D. Czyżewski, “Research on Luminance Distributions of Chip-On-Board Light-Emitting Diodes,” *Crystals*, vol. 9, no. 12, p. 645, Dec. 2019, doi: [10.3390/cryst9120645](https://doi.org/10.3390/cryst9120645).
- [5] A. Wiśniewski, “Calculations of energy savings using lighting control systems,” *Bull. Pol. Acad. Sci. Tech. Sci.*, vol. 68, no. 4, pp. 809–817, 2020, doi: [10.24425/bpasts.2020.134186](https://doi.org/10.24425/bpasts.2020.134186).
- [6] P. Pracki, “The impact of room and luminaire characteristics on general lighting in interiors,” *Bull. Pol. Acad. Sci. Tech. Sci.*, vol. 68, no. 3, pp. 447–457, 2020, doi: [10.24425/bpasts.2020.133372](https://doi.org/10.24425/bpasts.2020.133372).
- [7] D. Czyżewski, “Comparison of luminance distribution on the lighting surface of power LEDs,” *Photonics Lett. Pol.*, vol. 4, pp. 118–120, 2019.
- [8] S. Słomiński, “Advanced modelling and luminance analysis of LED optical systems,” *Bull. Pol. Acad. Sci. Tech. Sci.*, vol. 67, no. 6, pp. 1107–1116, 2019, doi: [10.24425/bpasts.2019.130886](https://doi.org/10.24425/bpasts.2019.130886).
- [9] S. Słomiński, “Selected problems in modern methods of luminance measurement of multisource led luminaires,” *Light Eng.*, vol. 24, no. 1, 2016.
- [10] S. Słomiński, “Typical Causes of Errors during Measuring Luminance Distributions in Relation to Glare Calculations,” *7th Light. Conf. Visegr. Countries, LUMEN V4 2018 – Proc.*, 2018, doi: [10.1109/LUMENV.2018.8521136](https://doi.org/10.1109/LUMENV.2018.8521136).
- [11] S. Slominski, “Potential resource of mistakes existing while using the modern methods of measurement and calculation in the glare evaluation,” *Proc. 2016 IEEE Light. Conf. Visegr. Countries, Lumen V4 2016*, 2016, doi: [10.1109/LUMENV.2016.7745538](https://doi.org/10.1109/LUMENV.2016.7745538).
- [12] TechnoTeam, “TechnoTeam Bildverarbeitung GmbH,” 2021. <https://www.technoteam.de/>.
- [13] C.A. Curcio, K.R. Sloan, R.E. Kalina, and A.E. Hendrickson, “Human photoreceptor topography,” *J. Comp. Neurol.*, vol. 292, no. 4, pp. 497–523, 1990, doi: [10.1002/cne.902920402](https://doi.org/10.1002/cne.902920402).
- [14] D.R. Williams, “Topography of the foveal cone mosaic in the living human eye,” *Vision Res.*, vol. 28, no. 3, pp. 433–454, Jan. 1988, doi: [10.1016/0042-6989\(88\)90185-X](https://doi.org/10.1016/0042-6989(88)90185-X).
- [15] B.A. Wandell, “The Photoreceptor Mosaic,” *Foundations of Vision*, Ch. 3, Stanford University, 1995. [Online] <https://foundationsofvision.stanford.edu/chapter-3-the-photoreceptor-mosaic> (accessed Feb. 27, 2022).
- [16] M.H. Pirenne, “Vision and the eye,” National Library of Australia. [Online] <https://catalogue.nla.gov.au/Record/2074379> (accessed Nov. 26, 2020).
- [17] E.A. Rossi and A. Roorda, “The relationship between visual resolution and cone spacing in the human fovea,” *Nat. Neurosci.*, vol. 13, no. 2, pp. 156–157, 2010, doi: [10.1038/nn.2465](https://doi.org/10.1038/nn.2465).
- [18] G.H. Scheir, P. Hanselaer, and W.R. Ryckaert, “Defining the Actual Luminous Surface in the Unified Glare Rating,” *LEUKOS – J. Illum. Eng. Soc.*, vol. 13, no. 4, pp. 201–210, 2017, doi: [10.1080/15502724.2017.1283232](https://doi.org/10.1080/15502724.2017.1283232).
- [19] R.D. Clear, “Discomfort glare: What do we actually know?,” *Light. Res. Technol.*, vol. 45, no. 2, pp. 141–158, 2013, doi: [10.1177/1477153512444527](https://doi.org/10.1177/1477153512444527).
- [20] Y. Tyukhova and C.E. Waters, “Discomfort Glare from Small, High-Luminance Light Sources When Viewed against a Dark Surround,” *LEUKOS – J. Illum. Eng. Soc.*, vol. 14, no. 4, pp. 215–230, 2018, doi: [10.1080/15502724.2018.1434415](https://doi.org/10.1080/15502724.2018.1434415).
- [21] S. Fotios and M. Kent, “Measuring Discomfort from Glare: Recommendations for Good Practice,” *LEUKOS – J. Illum. Eng. Soc.*, vol. 17, no. 4, pp. 338–358, 2021, doi: [10.1080/15502724.2020.1803082](https://doi.org/10.1080/15502724.2020.1803082).
- [22] G.H. Scheir, P. Hanselaer, P. Bracke, G. Deconinck, and W.R. Ryckaert, “Calculation of the Unified Glare Rating based on luminance maps for uniform and non-uniform light sources,” *Build. Environ.*, vol. 84, pp. 60–67, 2015, doi: [10.1016/j.buildenv.2014.10.027](https://doi.org/10.1016/j.buildenv.2014.10.027).
- [23] S. Jain, C. Karmann, and J. Wienold, “Behind electrochromic glazing: Assessing user’s perception of glare from the sun in a controlled environment,” *Energy Build.*, vol. 256, p. 111738, 2022, doi: [10.1016/j.enbuild.2021.111738](https://doi.org/10.1016/j.enbuild.2021.111738).
- [24] J.A. Yamin Garretón, E.M. Colombo, and A.E. Pattini, “A global evaluation of discomfort glare metrics in real office spaces with presence of direct sunlight,” *Energy Build.*, vol. 166, pp. 145–153, 2018, doi: [10.1016/j.enbuild.2018.01.024](https://doi.org/10.1016/j.enbuild.2018.01.024).
- [25] M. Kayakuş and I.S. Üncü, “Research Note: The measurement of road lighting with developed artificial intelligence software,” *Light. Res. Technol.*, vol. 51, no. 6, pp. 969–977, 2019, doi: [10.1177/1477153519825564](https://doi.org/10.1177/1477153519825564).
- [26] S. Safranek and R.G. Davis, “Sources of Error in HDRI for Luminance Measurement: A Review of the Literature,” *LEUKOS – J. Illum. Eng. Soc.*, vol. 17, no. 2, pp. 187–208, 2021, doi: [10.1080/15502724.2020.1721018](https://doi.org/10.1080/15502724.2020.1721018).
- [27] S. Słomiński, “Identification of the luminance measurements problems of multisources LED luminaires,” *Prz. Elektrotechniczny*, vol. 92, no. 7, p. 99590, 2016, doi: [10.15199/48.2016.07.43](https://doi.org/10.15199/48.2016.07.43).
- [28] C. Villa, R. Bremond, and E. Saint-Jacques, “Assessment of pedestrian discomfort glare from urban LED lighting,” *Light. Res. Technol.*, vol. 49, no. 2, pp. 147–172, 2017, doi: [10.1177/1477153516673402](https://doi.org/10.1177/1477153516673402).
- [29] Y. Yang, M. Ronnier, S.N. Ma, and X.Y. Liu, “Assessing glare. Part 1: Comparing uniform and non-uniform LED luminaires,” *Light. Res. Technol.*, vol. 49, no. 2, pp. 195–210, 2017, doi: [10.1177/1477153515607396](https://doi.org/10.1177/1477153515607396).
- [30] C. Pierson, “Discomfort glare from daylighting : influence of culture on discomfort glare perception,” no. October, 2017, doi: [10.25039/x44.2017.OP12](https://doi.org/10.25039/x44.2017.OP12).

- [31] S. Słomiński, "Identifying problems with luminaire luminance measurements for discomfort glare analysis," *Light. Res. Technol.*, vol. 48, no. 5, pp. 573–588, 2016, doi: [10.1177/1477153515596374](https://doi.org/10.1177/1477153515596374).
- [32] Commission Internationale de l'Éclairage. Discomfort Glare in Interior Lighting., "CIE Technical Report 117," Vienna: CIE, 1995.
- [33] C.-C. Sun, T.-X. Lee, S.-H. Ma, Y.-L. Lee, and S.-M. Huang, "Precise optical modeling for LED lighting verified by cross correlation in the midfield region," *Opt. Lett.*, vol. 31, no. 14, p. 2193, 2006, doi: [10.1364/ol.31.002193](https://doi.org/10.1364/ol.31.002193).
- [34] L. Simonot, F. Reux, S. Carré, and C. Martinsons, "The Usefulness of Near-Field Goniophotometry Data to Assess Illuminances and Discomfort Glare in Indoor Lighting," *LEUKOS – J. Illum. Eng. Soc. North Am.*, vol. 18, no. 2, pp. 246–257, 2021, doi: [10.1080/15502724.2021.1925129](https://doi.org/10.1080/15502724.2021.1925129).
- [35] C. Porsch, T. Walkling, A., Schmidt, F., Schierz, "Measurement of the Threshold Increment (Ti) in Road Lighting Based on Using IImd," *TechnoTeam Bild. GmbH*, [Online]. Available: www.technoteam.de.
- [36] "Konica Minolta LS-100/LS-110 catalog." https://www.konica-minolta.com/instruments/download/instruction_manual/light/pdf/ls-100-110_instruction_eng.pdf (accessed Jan. 23, 2022).
- [37] "Radiant Vision Systems," 2021. <https://www.radiantvisionsystems.com/>.
- [38] Comite Europeen de Normalisation, "PN-EN 13201: Road Lighting," 2016.
- [39] I.C. on I. (CIE), "Test Method for LED Lamps, LED Luminaires and LED Modules," *CIE S 025/E*, p. 59, 2015.
- [40] I.C. on I. (CIE), "Discomfort Caused by Glare from Luminaires with a Non-Uniform Source Luminance," *CIE 232*, p. 49, 2019, doi: [10.25039/TR.232.2019](https://doi.org/10.25039/TR.232.2019).
- [41] S. Ma, Y. Yang, M.R. Luo, and X. Liu, "Assessing and Modeling Discomfort Glare for Raw White LEDs with Different Patterns," *LEUKOS – J. Illum. Eng. Soc. North Am.*, vol. 13, no. 2, pp. 59–70, 2017, doi: [10.1080/15502724.2016.1252683](https://doi.org/10.1080/15502724.2016.1252683).
- [42] Y. Yang, M.R. Luo, and S.N. Ma, "Assessing glare. Part 2: Modifying Unified Glare Rating for uniform and non-uniform LED luminaires," *Light. Res. Technol.*, vol. 49, no. 6, pp. 727–742, 2017, doi: [10.1177/1477153516642622](https://doi.org/10.1177/1477153516642622).
- [43] Y. Yang, M.R. Luo, and W.J. Huang, "Assessing glare, Part 4: Generic models predicting discomfort glare of light-emitting diodes," *Light. Res. Technol.*, vol. 50, no. 5, pp. 739–756, 2018, doi: [10.1177/1477153516684375](https://doi.org/10.1177/1477153516684375).
- [44] S. Słomiński, "Luminance mapping to the light source model – possibilities to use a MML in the lighting technology field," *Prz. Elektrotechniczny*, vol. 87, no. 4, 2011.
- [45] S. Słomiński, "Digital luminance camera measurements of LED and luminaires – State of technology," *Prz. Elektrotechniczny*, vol. 91, no. 7, 2015, doi: [10.15199/48.2015.07.24](https://doi.org/10.15199/48.2015.07.24).
- [46] H. Hartridge, "Recent advances in the physiology of vision – part h," *Br. Med. J.*, vol. 1, no. 4512, pp. 913–916, 1947, doi: [10.1136/bmj.1.4512.913](https://doi.org/10.1136/bmj.1.4512.913).
- [47] B. O'BRIEN, "Vision and resolution in the central retina," *J. Opt. Soc. Am.*, vol. 41, no. 12, pp. 882–894, Dec. 1951, doi: [10.1364/JOSA.41.000882](https://doi.org/10.1364/JOSA.41.000882).
- [48] W.M.-C. physiology and evolution of vision in and U. 1979, "Ocular optical filtering," *Springer*, Accessed: Feb. 27, 2022. [Online]. Available: https://link.springer.com/chapter/10.1007/978-3-642-66999-6_3.
- [49] D.B. Farber, J.G. Flannery, R.N. Lolley, and D. Bok, "Distribution patterns of photoreceptors, protein, and cyclic nucleotides in the human retina," *Invest. Ophthalmol. Vis. Sci.*, vol. 26, no. 11, pp. 1558–1568, Nov. 1985.
- [50] C. Yuodelis and A. Hendrickson, "A qualitative and quantitative analysis of the human fovea during development," *Vision Res.*, vol. 26, no. 6, pp. 847–855, Jan. 1986, doi: [10.1016/0042-6989\(86\)90143-4](https://doi.org/10.1016/0042-6989(86)90143-4).
- [51] P.K. Ahnelt, H. Kolb, and R. Pflug, "Identification of a subtype of cone photoreceptor, likely to be blue sensitive, in the human retina," *J. Comp. Neurol.*, vol. 255, no. 1, pp. 18–34, 1987, doi: [10.1002/cne.902550103](https://doi.org/10.1002/cne.902550103).